HHS Public Access

Author manuscript

J Mol Biol. Author manuscript; available in PMC 2024 April 08.

Published in final edited form as:

J Mol Biol. 2019 July 26; 431(16): 3015–3027. doi:10.1016/j.jmb.2019.03.030.

Role of phenol-soluble modulins in *Staphylococcus epidermidis* biofilm formation and infection of indwelling medical devices

Katherine Y. Le[1,2], **Amer E. Villaruz**[1], **Yue Zheng**[1], **Lei He**[1,3], **Emilie L. Fisher**[1], **Thuan H. Nguyen**[1], **Trung V. Ho**[1], **Anthony J. Yeh**[1], **Hwang-Soo Joo**[1,#], **Gordon Y. C. Cheung**[1], **Michael Otto**[1,*]

[1]Pathogen Molecular Genetics Section, Laboratory of Bacteriology, National Institute of Allergy and Infectious Diseases, U.S. National Institutes of Health, 50 South Drive, Bethesda, Maryland 20814, USA

[2]Division of Hospital Internal Medicine, Department of Medicine, Mayo Clinic College of Medicine, 200 1st Street SW, Rochester, Minnesota 55902, USA

[3]Department of Laboratory Medicine, Renji Hospital, School of Medicine, Shanghai Jiaotong University, No. 160 Pujian Road, Shanghai 200127, China

Abstract

Phenol-soluble modulins (PSMs) are amphipathic, alpha-helical peptides that are secreted by staphylococci in high amounts in a quorum-sensing-controlled fashion. Studies performed predominantly in *Staphylococcus aureus* showed that PSMs structure biofilms, which results in reduced biofilm mass, while it has also been reported that *S. aureus* PSMs stabilize biofilms due to amyloid formation. We here analyzed the roles of PSMs in in-vitro and in-vivo biofilms of *Staphylococcus epidermidis*, the leading cause of indwelling device-associated biofilm infection. We produced isogenic deletion mutants for every *S. epidermidis psm* locus and a sequential deletion mutant in which production of all PSMs was abolished. In-vitro analysis substantiated the role of all PSMs in biofilm structuring. PSM-dependent biofilm expansion was not observed, in accordance with our finding that no *S. epidermidis* PSM produced amyloids. In a mouse model of indwelling device-associated infection, the total *psm* deletion mutant had a significant defect in dissemination. Notably, the total *psm* mutant produced a significantly more substantial biofilm on the implanted catheter than the wild-type strain. Our study, which for the first time directly quantified the impact of PSMs on biofilm expansion on an implanted device, shows that the in-vivo biofilm infection phenotype in *S. epidermidis* is in accordance with the PSM biofilm structuring and detachment model, which has important implications for the potential therapeutic application of quorum-sensing blockers.

Keywords

amyloids; device-associated infection; cyclophosphamide; neutrophils; quorum sensing

[*]Corresponding author: 50 South Drive, Bethesda, MD 20814, Fax: 301 402 0890, motto@niaid.nih.gov.
[#]Present address: Duksung Women's University, College of Natural Sciences, Department of Pre-PharmMed, 33 Samyang-ro 144-gil, Dobong-gu, Seoul 01369, South Korea

Declarations of interest: none

Introduction

Infection of indwelling medical devices is one of the leading types of nosocomial infections. These infections are often caused by opportunistic pathogens in patients that are immunocompromised due to underlying medical conditions or medical interventions such as surgery. Often, the infected device needs to be replaced, which leads to significantly increased costs for public health systems and a considerable burden for the patient. The main reason for the need to replace rather than treat the infected device with antibiotics stems from the fact that these infections commonly proceed with the development of biofilms, which are surface-attached bacterial aggregates that are inherently resistant to antibiotics [1–3].

Staphylococci are major nosocomial pathogens. *Staphylococcus epidermidis* in particular, an otherwise innocuous and even beneficial normal component of the skin microbiota, is the most frequent pathogen involved with device-associated infections [4, 5]. This situation has been explained by the facts that these bacteria are (i) abundant common inhabitants of human epithelia [6], and (ii) have exceptional ability to form biofilms [5, 7]. Biofilm-forming capacity has been linked to the variety and abundance of the molecules *S. epidermidis* secretes to attach to human matrix proteins and form a biofilm matrix [7]. Probably the most important components of the *S. epidermidis* biofilm matrix are the poly-N-acetylglucosamine polymeric exopolysaccharide PIA/PNAG [8] and the fibril-forming accumulation-associated protein Aap [9], as has been shown by both in-vitro and in-vivo research [10–12]. Some matrix proteins, such as Aap or the small basic protein (Sbp), form amyloid-like fibril scaffolds [13–15]. However, no molecule appears to be absolutely required for *S. epidermidis* biofilm formation. For example, isolates without the PIA/PNAG-encoding *ica* genes have been isolated from device-associated infections and *ica*-negative strains form in-vitro biofilms, although biofilms without PIA/PNAG are weaker [10, 16].

The formation of a mature biofilm, however, does not solely include biofilm matrix formation, but also requires structuring [17]. Biofilm-structuring forces lead to the formation of channels, which are deemed important for nutrient delivery throughout the biofilm, and thus to keep deeper biofilm layers alive. They also lead to detachment, which is a prerequisite for the systemic dissemination of a biofilm infection. In staphylococci, biofilm structuring has been linked to two molecule families: 1) enzymes that degrade biofilm matrix molecules, above all secreted proteases [18, 19], while enzymes that degrade PIA/PNAG are not known in staphylococci, and 2) the surfactant phenol-soluble modulin (PSM) peptides [20–23].

PSMs are peptides with pronounced amphipathy and α-helicity, properties that give them surfactant character [24, 25]. They are categorized into α- and β-type PSMs according to their length. The former are ~ 20 −25 and the latter ~ 45 amino acid in length. Every staphylococcal species produces a species-specific repertoire of PSMs, some but not all of which of share sequence similarities with homologous PSMs in other species. In-vitro research has shown that all PSMs of *S. aureus*, as well as the *S. epidermidis* PSMβ peptides, which are strongly produced in that species, structure biofilms. The same PSMs are so

far also the only bacterial factors for which roles in the in-vivo dissemination of biofilm-associated infection could be directly demonstrated [20, 21].

However, there are several important outstanding questions as for the role of PSMs in biofilms. First, the difficulties associated with producing isogenic deletion mutants in *S. epidermidis* has so far not allowed investigating the roles of PSMs other than the PSMβ peptides in *S. epidermidis*. Second, the effect that the absence of PSMs has on biofilm expansion, which is very pronounced in vitro, has so far not been analyzed in vivo on infected devices. Third, there is a model describing the role of PSMs in biofilm formation that to a certain extent contradicts that described above and which is based on the formation of amyloids by *S. aureus* PSMs in in-vitro setups [26]. While the role of PSM amyloids in *S. aureus* biofilm formation is controversial [27], whether *S. epidermidis* PSM form amyloids with a potential impact on biofilms has not yet been investigated. With some *S. epidermidis* PSMs showing higher similarity to amyloid-forming *S. aureus* PSMs (for example, *S. epidermidis* PSMδ to *S. aureus* PSMα3) than some of those to each other, amyloid formation by *S. epidermidis* PSMs appears possible and warrants investigation.

Therefore, we here put considerable efforts into the construction of isogenic mutants of the *psm* genes in *S. epidermidis*. Notably, we also constructed a total *psm* mutant, in which production of all PSMs of *S. epidermidis* is abolished. We tested the contribution of single and total mutants to in-vitro biofilm formation and also analyzed the contribution of PSMs to in-vivo biofilm formation and dissemination using the total PSM deletion strain and a mouse device-associated infection model. Our results demonstrate a significant contribution of all *S. epidermidis* PSMs to biofilm structuring processes and for the first time directly show that PSMs impact biofilm formation on an indwelling medical device in vivo. Furthermore, according to our results, *S. epidermidis* PSMs do not form amyloids and the PSM-dependent biofilm phenotypes *S. epidermidis* displays in-vitro and in-vivo are at odds with the predictions of the PSM amyloid model that was established in *S. aureus*.

Results

Production of psm deletion strains

S. epidermidis generally produces six PSMs: PSMα, PSMδ, PSMε, PSMβ1, PSMβ2, and the δ-toxin (sometimes called PSMγ) [25, 28–30]. The *psm*β operon contains three genes, coding for the PSMβ1 and PSMβ2 peptides, while the *psm*β3 gene appears not to be expressed, as we never found PSMβ3 production in any of many analyzed *S. epidermidis* culture filtrates. Sometimes, the *psm*β1 gene is duplicated, which is, however, not the case in the standard strain 1457 [31] that we and others have used for many previous studies and which we chose as the background strain to construct *psm* deletions. Further, *S. epidermidis* contains a homologue of the *S. aureus psm*α operon, but in which in contrast to *S. aureus*, only two peptides, PSMα and PSMδ, are encoded. PSMε is another α-type PSM that is encoded in a gene not connected with other *psm* genes. The δ-toxin is encoded within RNAIII, the intracellular effector of the accessory gene regulator (Agr) quorum-sensing system [32]. Agr strictly controls expression of all PSMs [33] (Fig. 1a,b).

We previously described an isogenic deletion mutant of the *psm*β operon, in which the *psm*β operon was replaced with a spectinomycin resistance cassette [20]. We also described an *hld* (δ-toxin) mutant, in which the *hld* start codon was changed to abolish production of δ-toxin without affecting RNAIII function [34]. Here, a strategy was used to produce markerless deletions of all other single *psm* genes. We also used that strategy, as described in methods, to produce a sequential total PSM deletion mutant on the basis of the spectinomycin-resistant *psm*β deletion mutant, in which all *psm* genes are completely deleted and *hld* expression is abolished (Fig. 1b). All mutants were verified for correct deletion by DNA sequencing as well as analysis of the PSM production pattern by reversed-phase high performance chromatography/electrospray ionization mass spectrometry (RP-HPLC/ESI-MS) (Fig. 1c). Mutations in *agr* that result in complete absence of PSM production happen frequently in the laboratory [35, 36]. Therefore, the correct PSM production pattern was verified at every step of the procedure. The total *psm* deletion strain (Δ*psm*), whose phenotype of complete PSM absence cannot be distinguished by this method from a spontaneous *agr* mutant, was verified as Agr-positive by analysis on milk agar plates, which assays for the maintained production of Agr-controlled proteases [37, 38].

Amyloid formation

We earlier described properties of pure *S. epidermidis* PSM peptides, such as capacities to lyse neutrophils [28]. We then did not analyze capacities to form amyloids, as amyloid formation by PSMs was only suggested and described later [26]. Therefore, we now subjected all pure *S. epidermidis* PSMs to the common thioflavin (ThT) test for amyloid formation. No PSM of *S. epidermidis* showed amyloid formation in this assay when tested at 0.1 mg/ml in physiological buffer conditions [10 mM sodium phosphate buffer (pH 8.0), 150 mM NaCl], whether diluted from DMSO stocks or pre-treated to destroy preformed amyloids, in contrast to amyloid-forming *S. aureus* PSMα3, which was used as control (Fig. 2a,b). As a further control, we treated all peptides with Tween 80, an amyloid-destroying agent, which led to abolishment of amyloid formation in the case of PSMα3, but did not alter fluorescence values, indicative of amyloid formation/destruction, with any *S. epidermidis* PSM. Thus, *S. epidermidis* PSMs do not form amyloids, at least under the tested conditions.

Role of S. epidermidis in in-vitro biofilms

There are many ways to analyze in-vitro biofilms. They can be categorized into two main setups: static and dynamic. In contrast to static models, dynamic models use flow, often applied in so-called flow cells, where fresh medium is run through the biofilm at a given flow rate [39]. Notably, no in-vitro model of biofilm formation can completely reflect the situation during infection, given the absence of host tissue formation, host matrix proteins, and immune defenses, to name but a few limitations. With this in mind, one could probably argue for either model, seen that device-associated infections occur in tissue or blood vessels, mimicking “static” or “dynamic” conditions, respectively. Thus, we used both a static and dynamic model to analyze the role of PSMs in in-vitro biofilms.

In the static model, we tested all single isogenic *psm* mutants as well as the total *psm* deletion strain (Δ*psm*). All showed significantly increased total and average biovolumes

and biofilm thickness, and a reduced roughness coefficient (Fig. 3). Average biovolume is a readout for the degree of channel formation, thus for the structuring capacity associated with PSMs (with a higher value meaning less structuring). All *S. epidermidis* PSMs showed the same general impact on biofilm formation that has been described by us previously for *S. aureus* PSMs and the *S. epidermidis* PSMβ peptides [20, 21]. Interestingly, we detected average biovolume and thickness values similar to those of the total *psm* deletion mutant even for deletion mutants of PSMs that are only produced in comparatively low amounts, such as PSMδ or PSMε. Contrastingly, total biovolume and roughness coefficients showed some differences that seemed correlated with PSM production levels, with the highly produced PSMβ peptides and δ-toxin showing the most pronounced effects. In the dynamic flow-cell model, we compared the total *psm* mutant with the wild-type *S. epidermidis* strain. Total and average biovolume as well as thickness were increased in the Δ*psm* versus the wild-type strain, while roughness was decreased (Fig. 4). These results thus reflected those achieved in the static model.

Role of PSMs in S. epidermidis biofilm-associated infection

As mentioned already above, in-vitro biofilm models only poorly reflect the conditions of biofilm-associated infection. Thus, to investigate the role of PSMs in biofilm-associated infection, we employed a frequently used mouse infection model, in which catheter pieces with attached bacteria are placed under the skin of mice [11, 40]. Most device-associated infections with *S. epidermidis* occur in immune-compromised patients [2]. Using a similar model, we previously showed that *S. epidermidis* causes increased severity of device-associated infection in severe combined immunodeficiency (SCID) mouse strains as compared to immunocompetent mice [41]. These mice are impaired in B- and/or T-cell responses, thus primarily in adaptive immunity. However, innate host defenses, and especially neutrophils, are generally known to have the most important impact on staphylococcal infections [42]. Therefore, we here first tested whether mice deficient in leukocytes develop device-associated infections with increased severity. Leukocytes were destroyed by treatment with cyclophosphamide (CY), which affects all cell types of myeloid origin [43].

We measured bacterial CFU on the inserted catheter, in the catheter-surrounding tissue, in several organs (spleen, liver, kidney), and lymph nodes to test for development of device-associated infection as well as its systemic dissemination. Biofilms on the implanted device were significantly larger, and significantly more CFU were detected in the surrounding tissue and all tested organs, as compared to non-CY-treated, immunocompetent mice (Fig. 5). Thus, leukocyte function has a significant impact on biofilm-associated device infection and its dissemination in mice.

We then used the same model under conditions of immune suppression to test for the role of PSMs using the total *psm* deletion mutant (Δ*psm*). Device-attached biofilms formed by the Δ*psm* mutant were significantly larger than those formed by wild-type *S. epidermidis*, while dissemination, as measured by CFU in the catheter-surrounding tissue, lymph nodes, and organs, was lower in mice infected with Δ*psm* bacteria. In the lymph nodes and liver, the differences were significant (Fig. 5).

Discussion

It is now well established that PSMs have a considerable impact on biofilm formation and represent major effectors of the previously described pronounced influence of Agr quorum-sensing regulation on staphylococcal biofilm development [17, 44, 45]. However, important questions have remained unanswered and there are contrasting schools of thought about how specific physico-chemical properties affect the biological functions of PSMs. First, except for our studies using a *psm*β deletion mutant [20], the impact of PSMs on *S. epidermidis* biofilms and biofilm infection has remained undefined. Second, whether there is biological relevance of PSM amyloid formation, in particular for biofilm formation and biofilm infections, has remained a matter of debate [27]. Finally, in the present study we also addressed whether leukocyte depletion has a significant impact on the severity of *S. epidermidis* device-associated infection. This represents an important question given that *S. epidermidis* is the major cause of device-associated infections, as well as device infection-associated bacteremia; and many patients that suffer from *S. epidermidis* infections are immunocompromised.

We showed previously that in a device-associated *S. epidermidis* mouse infection model similar to that used in the present study, CBSCBG-MM and Nu/Nu SCID mice, deficient in B- and T-cells, had ~ 5 – 10 times higher average CFU on infected catheters and surrounding tissue than wild-type mice [41]. Here, mice deficient in leukocytes, a major arm of innate immunity, showed an at least similarly pronounced deficiency in clearing *S. epidermidis* biofilm infection. We also measured dissemination to lymph nodes and into organs, which was increased at comparable rates. Thus, our results show that deficiency in leukocytes as major cellular mediators of innate immunity leads to significantly increased severity of experimental device-associated biofilm infection.

As for the role of PSMs, our results are in accordance with the general principle indicated in our previous studies using *S. aureus psm* mutants [21] and the *S. epidermidis psm*β mutant [20], inasmuch as dissemination into organs and establishment of second site infection was decreased in the absence of PSMs. However, we now also for the first time directly measured the extent of biofilm formation on the device. Our results show significantly increased biofilm formation on the device in the absence of PSMs, indicating in-vivo relevance of the model of PSM-mediated biofilm structuring and detachment in the used biofilm infection model.

While animal models or in-vitro flow-cell measurements of all single *psm* mutants would have required too large an amount of experiments, we tested all single *psm* mutants for their impact on static biofilm development. Some biofilm phenotypes showed a certain additivity of the effects of single PSMs; however, average biovolume and thickness values obtained for the total *psm* mutant were also reached by all single *psm* mutants. These observations reflect our previous findings using single *S. aureus psm* mutants [21]. They suggest that already the absence of PSMs that are expressed at comparatively low levels impacts biofilm phenotypes considerably, despite the continued presence of all other PSMs and an almost unchanged total PSM amount. We believe this may point to functional specification of PSMs with respect to their roles in biofilm structuring. Functional specification of PSMs is yet

poorly understood and testing the hypothesis that different PSMs have different functions in biofilm structuring remains an important task for future in-depth mechanistic research.

Our previous in-vitro studies have consistently shown that PSMs structure biofilms and their absence leads to biofilms with enhanced thickness but less channel formation [20, 21, 23]. Others have shown that some *S. aureus* PSMs (PSMα1, PSMα2, PSMα4, PSMβ1, PSMβ2) are contained in amyloid-like fibrils that lead to enhanced resistance of biofilms toward enzymatic degradation [26]. While we previously confirmed in-vitro aggregation and potential amyloid formation by several *S. aureus* PSMs [27], both our in-vitro and in-vivo analyses using *S. aureus psm* mutants indicated that this capacity does not have significant relevance for in-vitro or in-vivo biofilm formation [20, 21, 27]. We also recently provided experimental evidence for the attachment of *S. aureus* PSMs to DNA [27], indicating that the enhanced resistance of PSM-positive biofilms to degradation can be explained without the involvement of PSM amyloids. Here, we analyzed *S. epidermidis* PSMs for amyloid formation. In contrast to amyloid-forming *S. aureus* PSMα3, which was used as a control, no *S. epidermidis* PSM showed significant amyloid formation in an in-vitro assay. Furthermore, our in-vitro data achieved with *S. epidermidis psm* mutants support the model of PSM-mediated biofilm structuring and detachment. Finally, our analysis of in-vivo biofilm formation on an implanted device indicate that this model is in accordance with in-vivo phenotypes, at least under the in-vivo infection conditions tested in this study.

Recently, PSMα3 of *S. aureus* was shown to adapt an exceptional amyloid fibril structure, which was claimed to be linked to the functional properties of that peptide [46], in particular its cytolytic capacity, which is higher than that of most other tested PSMs [47]. We previously demonstrated that PSMδ of *S. epidermidis*, a homologue of the *S. aureus* PSMα peptides, has cytolytic capacities at least at the same level as those exhibited by PSMα3 [28]. It is thus of interest that PSMδ, similar to all other tested *S. epidermidis* PSMs, did not show amyloid formation. This result adds to previous evidence we obtained using an alanine screen peptide bank of PSMα3, which showed that several PSMα3 derivatives with abolished or strongly reduced amyloid-forming capacities maintained cytolytic activity, indicating that amyloid formation of PSMα3 is not linked to its cytolytic capacity [27]. Altogether, our data show that amyloid formation is not a general PSM feature and lend further support to the notion that the occasionally observed amyloid-like aggregation of PSMs does not have biological relevance, at least not for the phenotypes that have so far been described for PSMs.

Blocking quorum-sensing is a frequently proposed strategy of modern antivirulence drug development [48]. In *S. aureus*, the Agr quorum-sensing system controls a plethora of toxins [49]. These include PSMs, which are under exceptionally direct and strict regulation by Agr [33]. As we verified in the present study, all *S. epidermidis* PSMs are also under strict Agr control. While targeting Agr certainly appears a valuable strategy to treat acute, non-biofilm-associated infections, we previously noted that caution should be applied when evaluating quorum-sensing blocking as a potential therapeutic option for biofilm-associated infections [50]. Our present results show that the same caution should be applied for *S. epidermidis*, which is of particular importance given that biofilm-associated infection of medical devices is by far the most frequent type of infection that this opportunistic pathogen causes.

Then again, blocking Agr and thus, PSM production, according to our findings should diminish second-site infections. Future in-depth evaluation of quorum-sensing blockers for *S. epidermidis* infections should therefore include testing whether lowering the degree of biofilm formation on the device or the level of systemic dissemination is more important to achieve clinical improvement in such infections. Furthermore, *S. epidermidis* is a leading cause of nosocomial sepsis, an acute type of infection, for which quorum sensing blockers may be appropriate, a notion that remains to be tested.

Materials and methods

Bacterial strains and culture conditions

The *S. epidermidis* standard strain 1457 and its derivatives (see below) were used in all experiments (see Tab. 1 for a list of all strains). All strains were tested frequently, and always in pre-cultures of performed experiments, for the correct PSM production pattern and absence of Agr mutations (by RP-HPLC/MS or production of inhibition zones on proteolysis test plates). Cultures were grown in tryptic soy broth (TSB) or TSBg (TSB + 0.5% glucose), as indicated.

Gene deletion by allelic replacement

An allelic replacement procedure [51], was used to create markerless isogenic *psm*δ, and *psm*ε mutants in *S. epidermidis* 1457, a biofilm-forming clinical isolate frequently used for biofilm research [31]. First, ~1-kb regions upstream and downstream of the *psm* genes were amplified from *S. epidermidis* 1457 genomic DNA using PCR oligonucleotide pairs, introducing *attB1* and *attB2* sites at the distal ends (Tab. 2). The creation of the isogenic *psm*β mutant has been previously described [20]. Plasmids pKOR1-Δ*psm*δ and pKOR1-Δ*psm*ε lack the coding sequences for *psm*α, *psm*δ, and *psm*ε, respectively. Construction of the *hld* mutant (abolishing production of δ-toxin) has also been previously described [34]. In that strain, a start codon mutations was introduced (ATG to ATA) with pKOR1-Δ*hld*^{epi}, abolishing production of δ-toxin without interfering with the function of RNAIII, in whose gene it is embedded. The same strategy was used here to abolish production of PSMα (change of start codon of the *psm*α gene from ATG to ATA, using pKOR1-Δ*psm*α), as complete deletion of the gene proved to interfere with the production of PSMδ, whose gene is located downstream in the same operon.

The same allelic replacement procedure and plasmids were used to produce an isogenic quintuple (total) *psm* mutant in *S. epidermidis* 1457, with the exception of the *psm*α and *psm*δ genes. Since the *psm*α and *psm*δ genes are found on the same operon, a separate allelic replacement plasmid (pKOR1-Δ*psm*α/Δ*psm*δ) was constructed, which allowed for the simultaneous deletion of both genes. The isogenic quintuple *psm* mutant was then created sequentially as follows; an *hld* mutation was first introduced into the previously described isogenic *psm*β mutant [20] to generate an isogenic double *psm* mutant, Δ*psm*β/Δ*hld*. The genes for *psm*α and *psm*δ were then deleted with pKOR1-Δ*psm*α/Δ*psm*δ to generate a quadruple *psm* mutant (Δ*psm*β/Δ*hld*/Δ*psm*α/Δ*psm*δ). Finally, the quintuple isogenic *psm* mutant was created after allelic replacement with the pKOR1-Δ*psm*ε. The *S.*

epidermidis 1457 isogenic Δ*agr* mutant used in this study has been described previously [52]. All mutants carry an introduced spectinomycin resistance gene.

PSM detection and relative quantification

PSMs were detected using reversed-phase high performance liquid chromatography/ electrospray ionization mass spectrometry (RP-HPLC/ESI-MS) in principle as described [53] with some modifications, as described recently [54]. Obtained intensity values serve to quantify PSM production levels in a relative fashion. They can be used to directly compare the same PSM between different samples, and to a certain extent to compare with other PSMs of the same type, as intensity values for a given concentration are similar within PSMs of the α- and β-types.

Measurement of protease activity on proteolysis test plates

Protease activity was determined on skim-milk agar plates as described [37]. Two μl of bacterial cultures were dropped on the plates, which were incubated for 24 h at 37 °C.

Thioflavin T (ThT) assay for amyloid formation

The Thioflavin T (ThT) kit was purchased from AnaSpec [SensoLyte Thioflavin T β-Amyloid (1 – 42) Aggregation Kit]. *S. epidermidis* PSM peptides and *S. aureus* PSMα3 were prepared as 10 mg/ml stocks in DMSO and diluted for the ThT assay. Alternatively, they were subjected to pre-treatment with trifuoroacetic acid/hexafluoroisopropanol (1:1), as described [27] to abolish pre-formed amyloids. In each reaction, 0.1 mg/ml peptide was mixed with 200 μM ThT in 10 mM sodium phosphate buffer (pH 8.0) and 150 mM NaCl. For abolishment of amyloid formation, Tween 80 was added to a final concentration of 0.056%. The fluorescence of ThT was measured at 484 nm with excitation at 440 nm using a Tecan Spark multimode microplate reader every 5 min at 37 °C with 15 s shaking before each read.

In-vitro biofilm models

Wild-type and isogenic *S. epidermidis psm* deletion mutants were grown at 37 °C at 180 rotations per minute (rpm) to stationary growth phase. For static biofilm models, planktonic bacteria were vortexed and sonicated, and inoculated at an optical density (OD_{600}) of 0.1 in TSBg in Lab-Tek chambered cover glass plates and incubated at 37 °C for 48 h. After 48 h, growth media were removed and biofilms were gently washed with phosphate buffered saline (PBS). Stationary biofilms were then stained for 15 min at 37 °C in 4 μM propidium iodide (PI). For flow biofilm systems, planktonic wildtype and isogenic *psm* mutants were inoculated at an OD_{600} of 0.1 in TSBg to Stovall flow-cells and allowed to adhere to the glass surface at 37 °C for 6 h. Adherent bacterial biofilms were grown in constant flow (0.5 ml/min) of TSB containing 4 μM PI. At the end of the respective incubation periods, biofilms were gently washed with PBS, then resuspended in PBS, and imaged using confocal laser scanning microscopy (CLSM) on a Zeiss LSM710 confocal microscope. Image analyses were performed using Imaris and Comstat.

Animal model of device-associated infection

In-vivo studies were approved by the Institutional Animal Care and Use Committee of the NIAID. Animal work was performed adhering to the institution's guidelines for animal use, and followed the guidelines and basic principles in the United States Public Health Service Policy on Humane Care and Use of Laboratory Animals, and the Guide for the Care and Use of Laboratory Animals by certified staff in an Association for Assessment and Accreditation of Laboratory Animal Care (AAALAC) International accredited facility.

All C57BL/6J mice were female and six to eight weeks of age at the time of use. Mice were injected intraperitoneally with a 2-ml loading dose of cyclophosphamide (CY, 150 mg/kg, (immunosuppressed model) or saline (immunocompetent model) on day 1, and additional maintenance-doses of 2 ml of CY (100 mg/kg) or saline, respectively, on days 3, 5, and 7. Wild-type and isogenic *S. epidermidis psm* deletion mutant strains were grown at 37 °C at 180 rpm to stationary growth phase in TSB on day 7, inoculated to an OD_{600} of 0.1 in TSB from these pre-cultures on day 8 and grown to exponential growth phase at 37 °C at 180 rpm. Then, bacteria were centrifuged in a Sorvall Legend RT centrifuge (4150 rpm, 25°C, 15 min), after which the supernatants were decanted and the bacterial pellets were resuspended each in 10 ml of TSBg, vortexed and sonicated, and added to 1-cm segments of sterilized catheters (Terumo Surflash 14 gauge IV catheters). Catheter segments were incubated within the bacterial suspension for 2 h at 37 °C. Then, biofilm-coated catheters were gently washed with PBS and allowed to air dry. Catheters were subcutaneously inserted on the dorsa of mice under general anesthesia. Mice were monitored for 48 h and euthanized on day 10. Catheters, peri-catheter skin and soft tissues, lymph nodes (inguinal, axillary, brachial, superficial cervical), as well as distal organs (liver, kidney, spleen) were collected for determination of bacterial CFU. To that end, catheters were suspended in PBS, vortexed and sonicated as described [20], and serially diluted. Peri-catheter skin and soft tissues, lymph nodes, and distal organs were homogenized in PBS suspension with 2-mm borosilicate beads in a FastPrep 96 (MP Bio) homogenizer and serially diluted. Bacterial CFU were determined from serially diluted samples.

Statistics

Statistical evaluation was performed using Graph Pad Prism Version 7.01. Data were analyzed using 1-way ANOVA with Tukey's or Dunnett's multiple comparison tests for more than two groups, and unpaired Student's t-tests for the comparison of two groups. In-vivo data were subjected to Log10 transformation before analysis.

Acknowledgments

This study was supported by the Intramural Research Program of the National Institute of Allergy and Infectious Diseases (NIAID), U.S. National Institutes of Health (NIH) (project number 1 ZIA AI000904, to M.O.), The National Natural Science Foundation of China (grant 81501804, to L.H.), and the General Program of Shanghai Municipal Commission of Health and Family Planning (grant 20154Y0014, to L.H.).

Abbreviations:

Agr	accessory gene regulator

CFU	colony-forming units
CLSM	confocal laser scanning microscopy
PIA/PNAG	polysaccharide intercellular adhesin/poly-N-acetylglucosamine
PSM	phenol-soluble modulin
RP-HPLC/ESI-MS	high performance chromatography/electrospray ionization mass spectrometry
ThT	thioflavin

References

[1]. Darouiche RO. Device-associated infections: a macroproblem that starts with microadherence. Clin Infect Dis. 2001;33:1567–72. [PubMed: 11577378]

[2]. von Eiff C, Jansen B, Kohnen W, Becker K. Infections associated with medical devices: pathogenesis, management and prophylaxis. Drugs. 2005;65:179–214. [PubMed: 15631541]

[3]. Donlan RM, Costerton JW. Biofilms: survival mechanisms of clinically relevant microorganisms. Clin Microbiol Rev. 2002;15:167–93. [PubMed: 11932229]

[4]. Otto M *Staphylococcus epidermidis*--the 'accidental' pathogen. Nat Rev Microbiol. 2009;7:555–67. [PubMed: 19609257]

[5]. Zheng Y, He L, Asiamah TK, Otto M. Colonization of medical devices by staphylococci. Environ Microbiol. 2018;20:3141–53. [PubMed: 29633455]

[6]. Kloos WE, Musselwhite MS. Distribution and persistence of *Staphylococcus* and *Micrococcus* species and other aerobic bacteria on human skin. Appl Microbiol. 1975;30:381–5. [PubMed: 810086]

[7]. Otto M Staphylococcal biofilms. Curr Top Microbiol Immunol. 2008;322:207–28. [PubMed: 18453278]

[8]. Mack D, Fischer W, Krokotsch A, Leopold K, Hartmann R, Egge H, et al. The intercellular adhesin involved in biofilm accumulation of *Staphylococcus epidermidis* is a linear beta-1,6-linked glucosaminoglycan: purification and structural analysis. J Bacteriol. 1996;178:175–83. [PubMed: 8550413]

[9]. Hussain M, Herrmann M, von Eiff C, Perdreau-Remington F, Peters G. A 140-kilodalton extracellular protein is essential for the accumulation of *Staphylococcus epidermidis* strains on surfaces. Infect Immun. 1997;65:519–24. [PubMed: 9009307]

[10]. Schaeffer CR, Woods KM, Longo GM, Kiedrowski MR, Paharik AE, Buttner H, et al. Accumulation-associated protein enhances *Staphylococcus epidermidis* biofilm formation under dynamic conditions and is required for infection in a rat catheter model. Infect Immun. 2015;83:214–26. [PubMed: 25332125]

[11]. Rupp ME, Ulphani JS, Fey PD, Bartscht K, Mack D. Characterization of the importance of polysaccharide intercellular adhesin/hemagglutinin of *Staphylococcus epidermidis* in the pathogenesis of biomaterial-based infection in a mouse foreign body infection model. Infect Immun. 1999;67:2627–32. [PubMed: 10225932]

[12]. Rupp ME, Ulphani JS, Fey PD, Mack D. Characterization of *Staphylococcus epidermidis* polysaccharide intercellular adhesin/hemagglutinin in the pathogenesis of intravascular catheter-associated infection in a rat model. Infect Immun. 1999;67:2656–9. [PubMed: 10225938]

[13]. Conrady DG, Brescia CC, Horii K, Weiss AA, Hassett DJ, Herr AB. A zinc-dependent adhesion module is responsible for intercellular adhesion in staphylococcal biofilms. Proc Natl Acad Sci U S A. 2008;105:19456–61. [PubMed: 19047636]

[14]. Decker R, Burdelski C, Zobiak M, Buttner H, Franke G, Christner M, et al. An 18 kDa scaffold protein is critical for *Staphylococcus epidermidis* biofilm formation. PLoS Pathog. 2015;11:e1004735. [PubMed: 25799153]

[15]. Wang Y, Jiang J, Gao Y, Sun Y, Dai J, Wu Y, et al. *Staphylococcus epidermidis* small basic protein (Sbp) forms amyloid fibrils, consistent with its function as a scaffolding protein in biofilms. J Biol Chem. 2018;293:14296–311. [PubMed: 30049797]

[16]. Rohde H, Burandt EC, Siemssen N, Frommelt L, Burdelski C, Wurster S, et al. Polysaccharide intercellular adhesin or protein factors in biofilm accumulation of *Staphylococcus epidermidis* and *Staphylococcus aureus* isolated from prosthetic hip and knee joint infections. Biomaterials. 2007;28:1711–20. [PubMed: 17187854]

[17]. Otto M Staphylococcal infections: mechanisms of biofilm maturation and detachment as critical determinants of pathogenicity. Annu Rev Med. 2013;64:175–88. [PubMed: 22906361]

[18]. Boles BR, Horswill AR. Staphylococcal biofilm disassembly. Trends Microbiol. 2011;19:449–55. [PubMed: 21784640]

[19]. Loughran AJ, Atwood DN, Anthony AC, Harik NS, Spencer HJ, Beenken KE, et al. Impact of individual extracellular proteases on *Staphylococcus aureus* biofilm formation in diverse clinical isolates and their isogenic *sarA* mutants. Microbiologyopen. 2014;3:897–909. [PubMed: 25257373]

[20]. Wang R, Khan BA, Cheung GY, Bach TH, Jameson-Lee M, Kong KF, et al. *Staphylococcus epidermidis* surfactant peptides promote biofilm maturation and dissemination of biofilm-associated infection in mice. J Clin Invest. 2011;121:238–48. [PubMed: 21135501]

[21]. Periasamy S, Joo HS, Duong AC, Bach TH, Tan VY, Chatterjee SS, et al. How *Staphylococcus aureus* biofilms develop their characteristic structure. Proc Natl Acad Sci U S A. 2012;109:1281–6. [PubMed: 22232686]

[22]. Otto M Phenol-soluble modulins. Int J Med Microbiol. 2014;304:164–9. [PubMed: 24447915]

[23]. Dastgheyb SS, Villaruz AE, Le KY, Tan VY, Duong AC, Chatterjee SS, et al. Role of Phenol-Soluble Modulins in Formation of *Staphylococcus aureus* Biofilms in Synovial Fluid. Infect Immun. 2015;83:2966–75. [PubMed: 25964472]

[24]. Peschel A, Otto M. Phenol-soluble modulins and staphylococcal infection. Nat Rev Microbiol. 2013;11:667–73. [PubMed: 24018382]

[25]. Cheung GY, Joo HS, Chatterjee SS, Otto M. Phenol-soluble modulins--critical determinants of staphylococcal virulence. FEMS Microbiol Rev. 2014;38:698–719. [PubMed: 24372362]

[26]. Schwartz K, Syed AK, Stephenson RE, Rickard AH, Boles BR. Functional amyloids composed of phenol soluble modulins stabilize *Staphylococcus aureus* biofilms. PLoS Pathog. 2012;8:e1002744. [PubMed: 22685403]

[27]. Zheng Y, Joo HS, Nair V, Le KY, Otto M. Do amyloid structures formed by *Staphylococcus aureus* phenol-soluble modulins have a biological function? Int J Med Microbiol. 2018;308:675–82. [PubMed: 28867522]

[28]. Cheung GY, Rigby K, Wang R, Queck SY, Braughton KR, Whitney AR, et al. *Staphylococcus epidermidis* strategies to avoid killing by human neutrophils. PLoS Pathog. 2010;6:e1001133. [PubMed: 20949069]

[29]. Mehlin C, Headley CM, Klebanoff SJ. An inflammatory polypeptide complex from *Staphylococcus epidermidis*: isolation and characterization. J Exp Med. 1999;189:907–18. [PubMed: 10075974]

[30]. Yao Y, Sturdevant DE, Otto M. Genomewide analysis of gene expression in *Staphylococcus epidermidis* biofilms: insights into the pathophysiology of *S. epidermidis* biofilms and the role of phenol-soluble modulins in formation of biofilms. J Infect Dis. 2005;191:289–98. [PubMed: 15609240]

[31]. Mack D, Siemssen N, Laufs R. Parallel induction by glucose of adherence and a polysaccharide antigen specific for plastic-adherent *Staphylococcus epidermidis*: evidence for functional relation to intercellular adhesion. Infect Immun. 1992;60:2048–57. [PubMed: 1314224]

[32]. Novick RP, Ross HF, Projan SJ, Kornblum J, Kreiswirth B, Moghazeh S. Synthesis of staphylococcal virulence factors is controlled by a regulatory RNA molecule. EMBO J. 1993;12:3967–75. [PubMed: 7691599]

[33]. Queck SY, Jameson-Lee M, Villaruz AE, Bach TH, Khan BA, Sturdevant DE, et al. RNAIII-independent target gene control by the agr quorum-sensing system: insight into the evolution of virulence regulation in *Staphylococcus aureus*. Mol Cell. 2008;32:150–8. [PubMed: 18851841]

[34]. Nakamura Y, Oscherwitz J, Cease KB, Chan SM, Munoz-Planillo R, Hasegawa M, et al. *Staphylococcus* delta-toxin induces allergic skin disease by activating mast cells. Nature. 2013;503:397–401. [PubMed: 24172897]

[35]. Somerville GA, Beres SB, Fitzgerald JR, DeLeo FR, Cole RL, Hoff JS, et al. In vitro serial passage of *Staphylococcus aureus*: changes in physiology, virulence factor production, and *agr* nucleotide sequence. J Bacteriol. 2002;184:1430–7. [PubMed: 11844774]

[36]. Villaruz AE, Bubeck Wardenburg J, Khan BA, Whitney AR, Sturdevant DE, Gardner DJ, et al. A point mutation in the *agr* locus rather than expression of the Panton-Valentine leukocidin caused previously reported phenotypes in *Staphylococcus aureus* pneumonia and gene regulation. J Infect Dis. 2009;200:724–34. [PubMed: 19604047]

[37]. Vuong C, Gotz F, Otto M. Construction and characterization of an *agr* deletion mutant of *Staphylococcus epidermidis*. Infect Immun. 2000;68:1048–53. [PubMed: 10678906]

[38]. Yao Y, Vuong C, Kocianova S, Villaruz AE, Lai Y, Sturdevant DE, et al. Characterization of the *Staphylococcus epidermidis* accessory-gene regulator response: quorum-sensing regulation of resistance to human innate host defense. J Infect Dis. 2006;193:841–8. [PubMed: 16479519]

[39]. Malone M, Goeres DM, Gosbell I, Vickery K, Jensen S, Stoodley P. Approaches to biofilm-associated infections: the need for standardized and relevant biofilm methods for clinical applications. Expert Rev Anti Infect Ther. 2017;15:147–56. [PubMed: 27858472]

[40]. Kadurugamuwa JL, Sin LV, Yu J, Francis KP, Purchio TF, Contag PR. Noninvasive optical imaging method to evaluate postantibiotic effects on biofilm infection in vivo. Antimicrob Agents Chemother. 2004;48:2283–7. [PubMed: 15155235]

[41]. Vuong C, Kocianova S, Yu J, Kadurugamuwa JL, Otto M. Development of real-time in vivo imaging of device-related *Staphylococcus epidermidis* infection in mice and influence of animal immune status on susceptibility to infection. J Infect Dis. 2008;198:258–61. [PubMed: 18491976]

[42]. Rigby KM, DeLeo FR. Neutrophils in innate host defense against *Staphylococcus aureus* infections. Semin Immunopathol. 2012;34:237–59. [PubMed: 22080185]

[43]. Hall AG, Tilby MJ. Mechanisms of action of, and modes of resistance to, alkylating agents used in the treatment of haematological malignancies. Blood Rev. 1992;6:163–73. [PubMed: 1422285]

[44]. Joo HS, Otto M. Molecular basis of in vivo biofilm formation by bacterial pathogens. Chem Biol. 2012;19:1503–13. [PubMed: 23261595]

[45]. Le KY, Dastgheyb S, Ho TV, Otto M. Molecular determinants of staphylococcal biofilm dispersal and structuring. Front Cell Infect Microbiol. 2014;4:167. [PubMed: 25505739]

[46]. Tayeb-Fligelman E, Tabachnikov O, Moshe A, Goldshmidt-Tran O, Sawaya MR, Coquelle N, et al. The cytotoxic *Staphylococcus aureus* PSMalpha3 reveals a cross-alpha amyloid-like fibril. Science. 2017;355:831–3. [PubMed: 28232575]

[47]. Wang R, Braughton KR, Kretschmer D, Bach TH, Queck SY, Li M, et al. Identification of novel cytolytic peptides as key virulence determinants for community-associated MRSA. Nat Med. 2007;13:1510–4. [PubMed: 17994102]

[48]. Dickey SW, Cheung GYC, Otto M. Different drugs for bad bugs: antivirulence strategies in the age of antibiotic resistance. Nat Rev Drug Discov. 2017;16:457–71. [PubMed: 28337021]

[49]. Le KY, Otto M. Quorum-sensing regulation in staphylococci-an overview. Front Microbiol. 2015;6:1174. [PubMed: 26579084]

[50]. Kong KF, Vuong C, Otto M. *Staphylococcus* quorum sensing in biofilm formation and infection. Int J Med Microbiol. 2006;296:133–9. [PubMed: 16487744]

[51]. Bae T, Schneewind O. Allelic replacement in *Staphylococcus aureus* with inducible counter-selection. Plasmid. 2006;55:58–63. [PubMed: 16051359]

[52]. Vuong C, Gerke C, Somerville GA, Fischer ER, Otto M. Quorum-sensing control of biofilm factors in *Staphylococcus epidermidis*. J Infect Dis. 2003;188:706–18. [PubMed: 12934187]

[53]. Joo HS, Otto M. The isolation and analysis of phenol-soluble modulins of *Staphylococcus epidermidis*. Methods Mol Biol. 2014;1106:93–100. [PubMed: 24222457]

[54]. Piewngam P, Zheng Y, Nguyen TH, Dickey SW, Joo HS, Villaruz AE, et al. Pathogen elimination by probiotic *Bacillus* via signalling interference. Nature. 2018;562:532–7. [PubMed: 30305736]

[55]. Chatterjee SS, Joo HS, Duong AC, Dieringer TD, Tan VY, Song Y, et al. Essential *Staphylococcus aureus* toxin export system. Nat Med. 2013;19:364–7. [PubMed: 23396209]

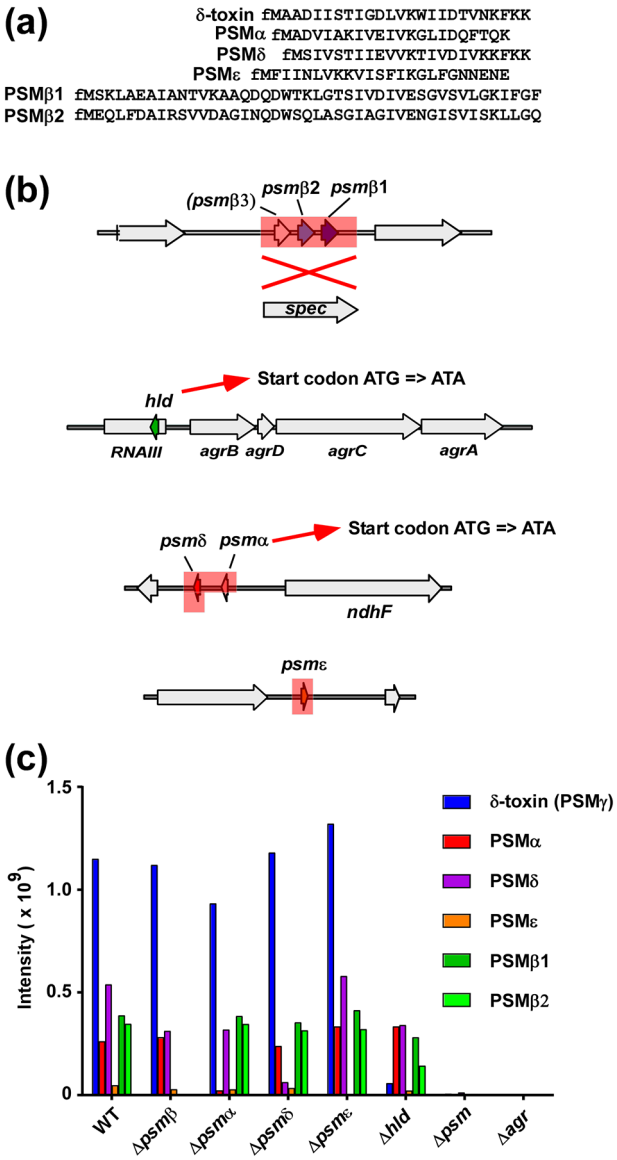

Fig. 1. *S. epidermidis* PSMs and construction of isogenic *psm* deletion mutants.

(**a**) Amino acid sequences of *S. epidermidis* PSMs. Note all PSMs have an N-terminal formylated methionine (fM) due to export by a dedicated ABC transporter without a signal peptide [55]. (**b**) *S. epidermidis psm* deletion mutants. The *psm*β deletion mutant was constructed by replacement of the entire *psm*β operon with a spectinomycin resistance cassette. Note the hypothetical PSMβ3 peptide does not appear to be produced. The quintuple (total) *psm* deletion mutants was then constructed by sequential deletion of the other *psm* loci, in the order as shown from top to bottom. Single *psm* deletion mutants were also constructed. In the case of *hld* (encoding δ-toxin) and *psm*α, start codon mutations were introduced instead of complete gene deletions, so as not to interfere with production of RNAIII or expression of *psm*δ, respectively. Deleted or replaced sections are shadowed in red. (**c**) Analysis of PSM production pattern by RP-HPLC/MS of all *psm* mutants used in thus study.

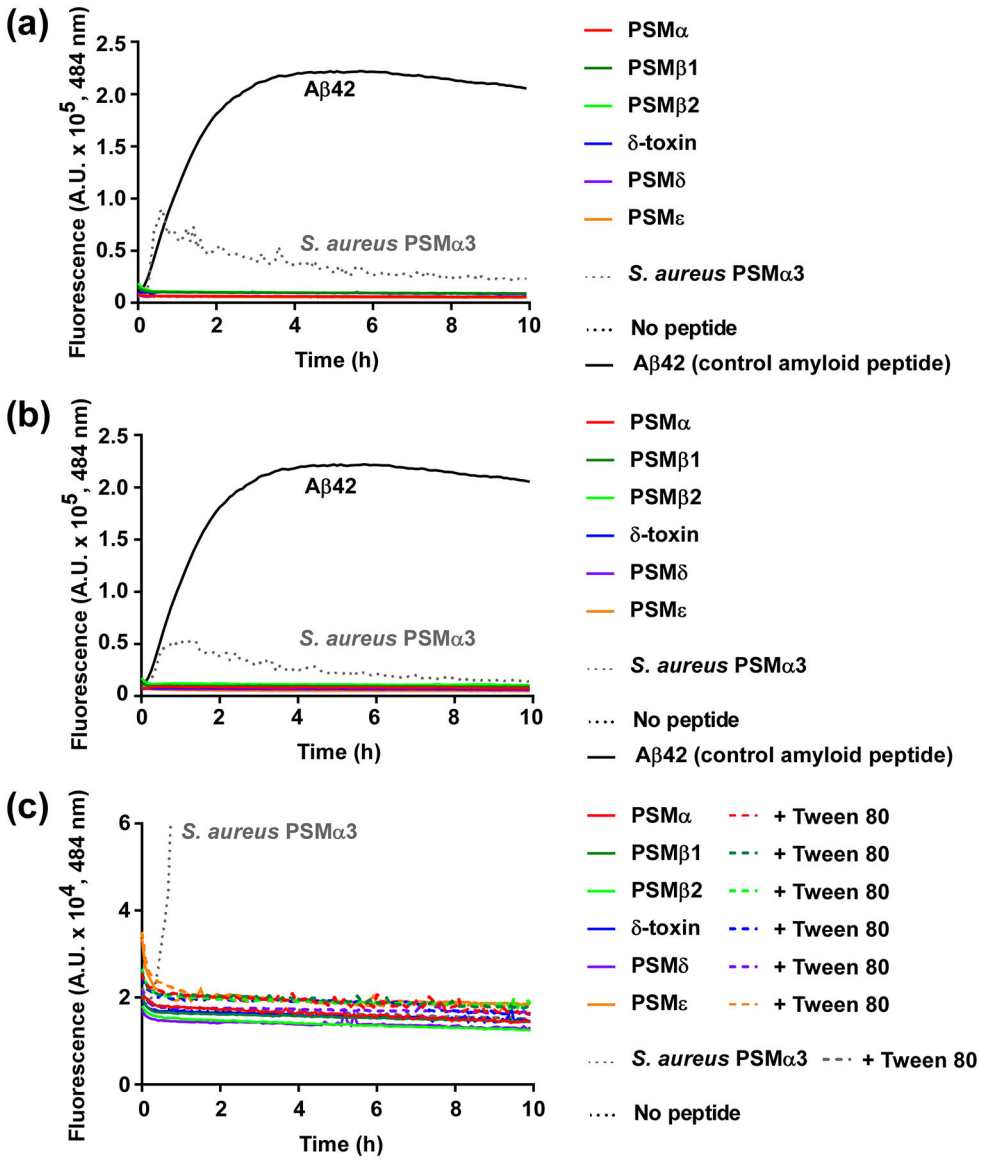

Fig. 2. Test for amyloid formation of *S. epidermidis* PSMs.

All *S. epidermidis* PSMs, as well as *S. aureus* PSMα3 and the control amyloid peptide Aβ42, were subjected to a ThT amyloid formation assay at a final concentration of 0.1 mg/ml in 10 mM sodium phosphate buffer (pH 8.0)/150 mM NaCl. The amyloid-indicative fluorescence at 484 nm was measured over 10 h. (**a**) Assay with PSM peptides diluted 1:100 from 10-mg/ml stocks in 100% DMSO. (**b**) Assay with PSM peptides pre-treated to abolish pre-formed amyloids using trifluoroacetic acid/hexafluoroisopropanol (1:1). (**c**) Assay comparing peptides pre-treated as in (**b**) with or without addition of Tween 80 to destroy pre-formed amyloids.

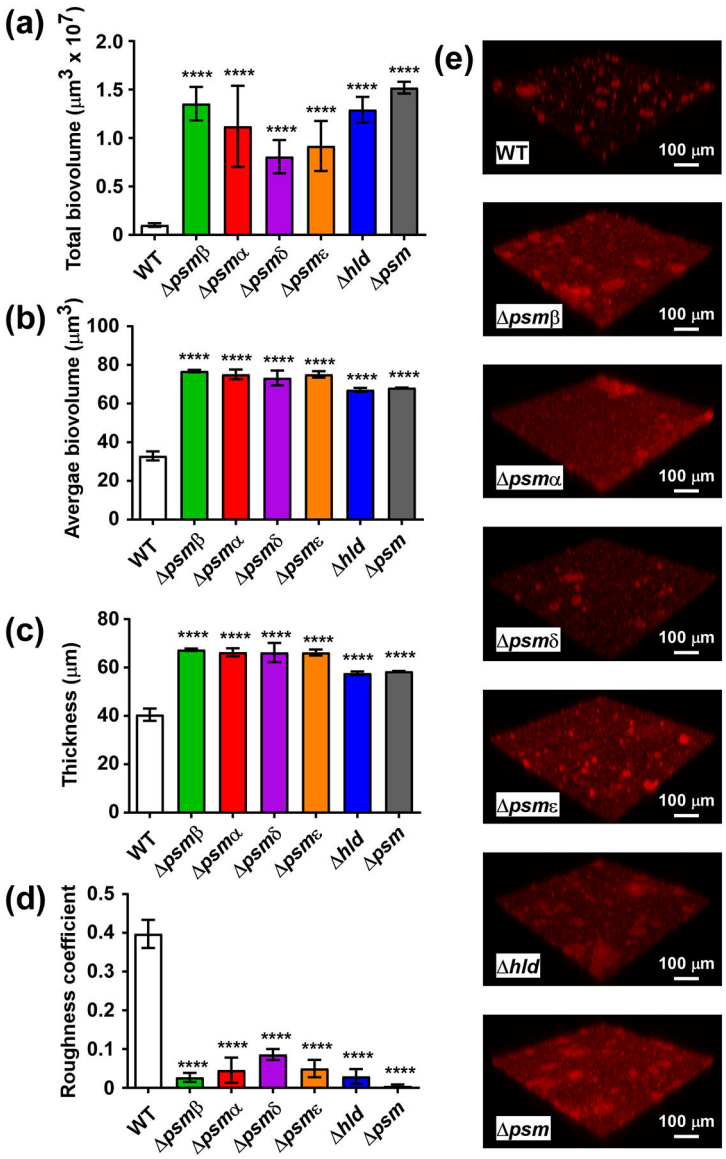

Fig. 3. Static in-vitro biofilm formation by single and total *S. epidermidis psm* mutants.

Biofilms were grown in TSBg in static mode for 48 h, measured by CLSM, and analyzed by Imaris or Comstat software. In addition to *psm* mutants, an isogenic mutant of the quorum-sensing *psm* control system *agr* was measured. (**a**) Total biovolumes (total biofilm mass). (**b**) Average biovolumes (More compact biofilm have higher; biofilms with more channel formation lower values.) (**c**) Thickness. (**d**) Roughness coefficient (Biofilms that are smoother have a lower value.) (**e**) Representative CLSM example pictures. (**a-d**) ****, $p<0.0001$ [1-way ANOVA with Dunnett's post-test versus data obtained with the wild-type (WT) strain]. Data are from n=16 measurements of randomly selected areas in a sample. The experiment was repeated with similar results.

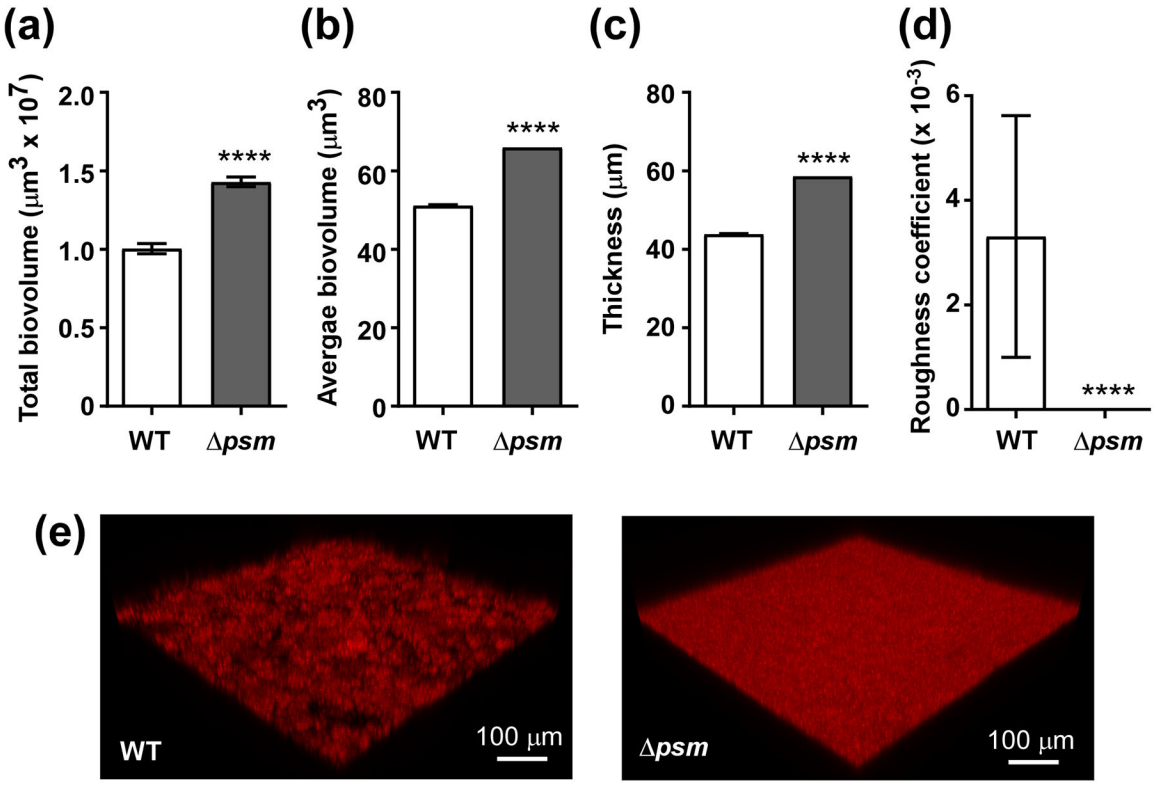

Fig. 4. Dynamic in-vitro biofilm formation by wild-type and isogenic Δ*psm* mutants strains.

Biofilms were grown in TSBg in dynamic mode in flow cells for 48 h, measured by CLSM, and analyzed by Imaris or Comstat software. (**a**) Total biovolumes (total biofilm mass). (**b**) Average biovolumes (More compact biofilm have higher; biofilms with more channel formation lower values.) (**c**) Thickness. (**d**) Roughness coefficient (Biofilms that are smoother have a lower value.) (**e**) Representative CLSM example pictures. (**a-d**) ****, $p<0.0001$ (unpaired t-tests). Data are from n=15 measurements of randomly selected areas in a sample. The experiment was repeated with similar results.

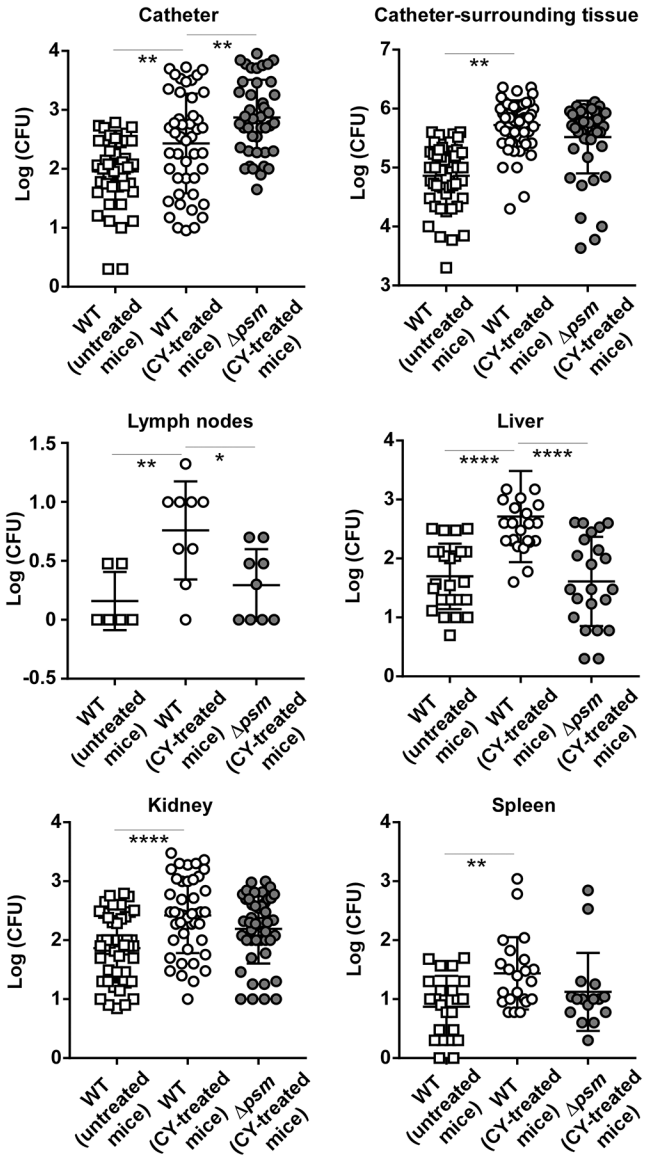

Fig. 5. Biofilm-associated device infection model.

Catheter pieces coated with equal amounts of wild-type or Δ*psm* bacteria were inserted subcutaneously into the dorsa of mice, which were treated with cyclophosphamide to obtain leukocyte-deficient immune suppression. Another group of mice infected with wild-type *S. epidermidis*-coated catheters received saline as control to maintain immune competency. All groups consisted of n=26 mice with two inserted catheters each, resulting in n=52 data points. Occasionally, catheters fell out and were not included in the counting. For organs and lymph nodes, only data points are shown in case bacteria were detected. Especially in lymph nodes, detection of bacteria was rare. *, $p<0.05$; **, $p<0.01$; ****, $p<0.0001$ [1-way ANOVA with Tukey's post-test. Only comparisons between untreated versus CY-treated, and CY-treated mice infected with wild-type (WT) versus Δ*psm S. epidermidis* are shown.]

Table 1.

Strains used in this study

Strains/plasmids	Relevant genotype and property	Source
S. aureus strains		
RN4220	Derived from NCTC8325–4; $r^{-}m^{+}$	[52]
S. epidermidis strains		
1457	Clinical biofilm-forming wild-type strain	[28]
1457 Δ*psm*α	Isogenic start codon (ATG to ATA) *psm*α mutant of 1457	This study
1457 Δ*psm*β	Isogenic *psm*β deletion mutant of 1457; *psm*β operon replaced with spectinomycin resistance cassette; $spec^{R}$	[17]
1457 Δ*hld*	Isogenic *hld* start codon mutant (ATG to ATA) of 1457; Hld (δ-toxin) protein production abolished without interfering with the function of RNAIII	[31]
1457 Δ*psm*ε	Isogenic markerless *psm*ε deletion mutant of 1457	This study
1457 Δ*psm*δ	Isogenic markerless *psm*δ deletion mutant of 1457	This study
1457 Δ*psm*	Quintuple (total) isogenic *psm* mutant of 1457 (Δ*psm*β/Δ*hld*/Δ*psm*α/Δ*psm*δ/Δ*psm*ε)	This study
1457 Δ*agr*	Isogenic *agr* deletion mutant of 1457	[49]
E. coli strains		
DH5α	*endA*1 *recA*1 *gyrA*96 *thi-1 hsdR17*(r_{K}^{-} m_{K}^{+}) *relA*1 *supE*44 (*lacZYA-argF*) U169 F- 80d*lacZ*M15 *deoR phoA*	Invitrogen

Table 2.

Oligonucleotides used in this study

Name	Sequence
For isogenic *psm*α/*psm*δ deletion mutant	
*psm*α.δ-att1	GGGGACAAGTTTGTACAAAAAAGCAGGCTTCACAAATAATGTTGCACCCCAAAACATGGTCAT
*psm*α.δ-rev1	TGTCCCAGGCCCATGTAGAACCCTTACTAATTTGTTATCTATAGTGTAACTGGAAT
*psm*α.δ-rev2	TTCTACATGGGCCTGGGACATAATTCCTATC
*psm*α.δ-att2	GGGGACCACTTTGTACAAGAAAGCTGGGTTCATAAATGTGGCATCGTGATCTGTTTTAGAATAA
For isogenic *psm*ε deletion mutant	
*psm*ε-att1	GGGGACAAGTTTGTACAAAAAAGCAGGCTTTTCAAAAAGATTTTTTACTACAAATATAATAGAATTAACA
*psm*ε-rev1	GAGGGGCGGAGTAGAGAATACACCTCCTATGTATTTGTTAACTAAATTATAGTATTGAAC
*psm*ε-rev2	TATTCTCTACTCCGCCCCTCCTGTTAGAGG
*psm*ε-att1	GGGGACCACTTTGTACAAGAAAGCTGGGTACCCTAGACCTGTTGAAAGTGGCATTATGA
For isogenic *psm*α start codon change mutant	
*psm*α-att1	GGGGACAAGTTTGTACAAAAAAGCAGGCTTCACAAATAATGTTGCACCCCAAAACATGGTCAT
*psm*α-rev1	AGGGAGGTCATTTAAATAGCAGATGTAATC
*psm*α-rev2	ATTACATCTGCTATTTAAATGACCTCCCTT
*psm*α-att2	GGGGACCACTTTGTACAAGAAAGCTGGGTTCATAAATGTGGCATCGTGATCTGTTTTAGAATAA
For isogenic *psm*δ deletion mutant	
*psm*δ-att1	GGGGACAAGTTTGTACAAAAAAGCAGGCTTCACAAATAATGTTGCACCCCAAAACATGGTCAT
*psm*δ-rev1	TGTCCCAGGCCCATGTAGAATCCTTTCAAAAGGGAAATGTATTTAGAGATG
*psm*δ-rev2	TTCTACATGGGCCTGGGACATAATTCCTATC
*psm*δ-att2	GGGGACCACTTTGTACAAGAAAGCTGGGTTCATAAATGTGGCATCGTGATCTGTTTTAGAATAA